

# A series of novel, selective matriptase inhibitors

Dawid Dębowski<sup>1</sup>, Aleksandra Helbik-Maciejewska<sup>1</sup>, Agata Gitlin-Domagalska<sup>1</sup>, Malihe Hassanzadeh<sup>2</sup>, Antoine Désilets<sup>2</sup>, Pierre-Luc Boudreault<sup>2</sup>, Richard Leduc<sup>2</sup>, Anna Łęgowska<sup>1</sup>, Krzysztof Rolka<sup>1</sup>

<sup>1</sup> Department of Molecular Biochemistry, Faculty of Chemistry, University of Gdansk, Gdansk, Poland;

<sup>2</sup> Faculty of Medicine and Health Sciences, and Institut de Pharmacologie de Sherbrooke Université de Sherbrooke, Sherbrooke, Québec (Canada)

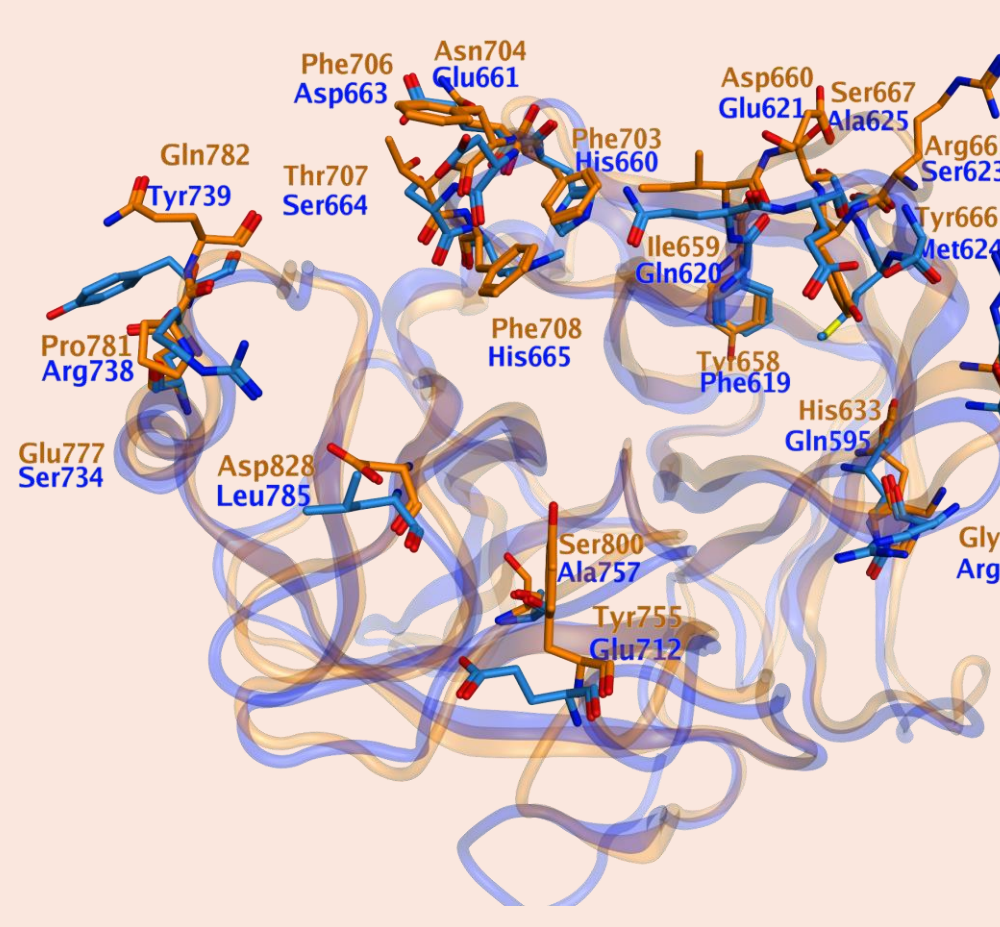


## BACKGROUND

## OBJECTIVES

Even though both type II transmembrane serine proteases (TTSPs), matriptase-1 (MT1) and matriptase-2 (MT2) share significant structural similarity and substrate specificity, they differ in biological functions [1].

- MT1**
- widely expressed in all types of epithelial tissues
  - maintains integrity of epithelial tissues
  - increased expression reported in epithelial cancers
  - in breast and prostate cancers increased expression is considered as a predictive factor of poor disease prognosis
- MT2**
- mostly localized in the liver
  - regulates iron homeostasis
  - differently from MT1, a positive correlation between its increased level and prognosis in the breast cancer patients



MT1-MT2 active site superimposition

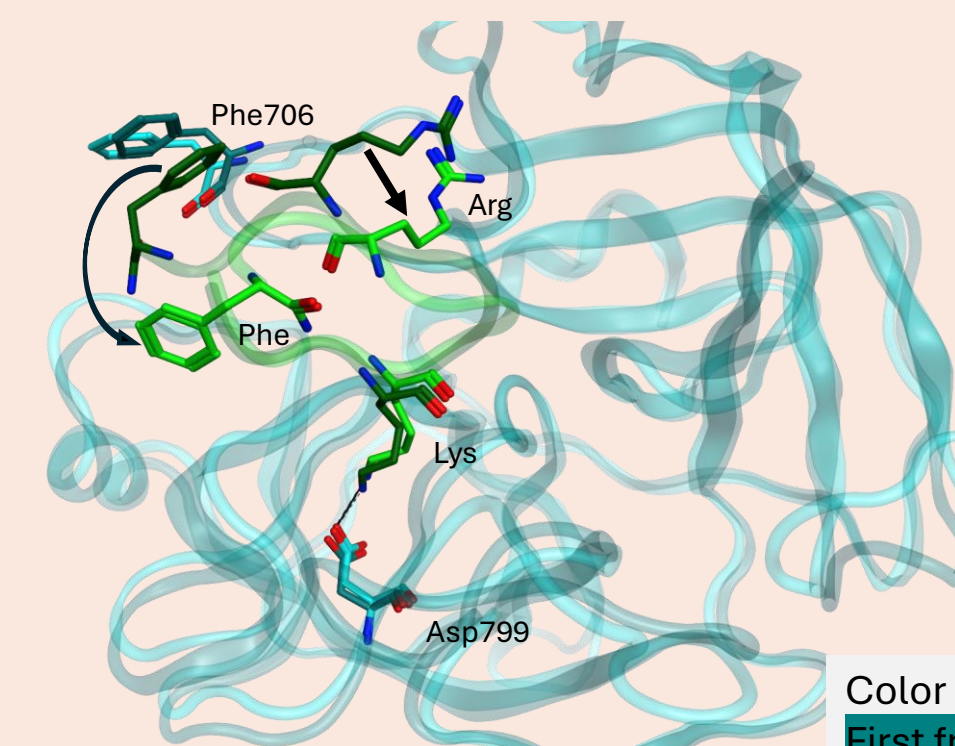
We have shown recently, that the gradual shortening of the primary structure of Chinese frog-skin derived inhibitor (HV-BBI, *Huia versabilis* Bowman-Birk inhibitor, 18-amino acids) led to strong non-covalent, disulfide-bridged MT1 inhibitor (13-amino acids) with C-terminal amide group [2].



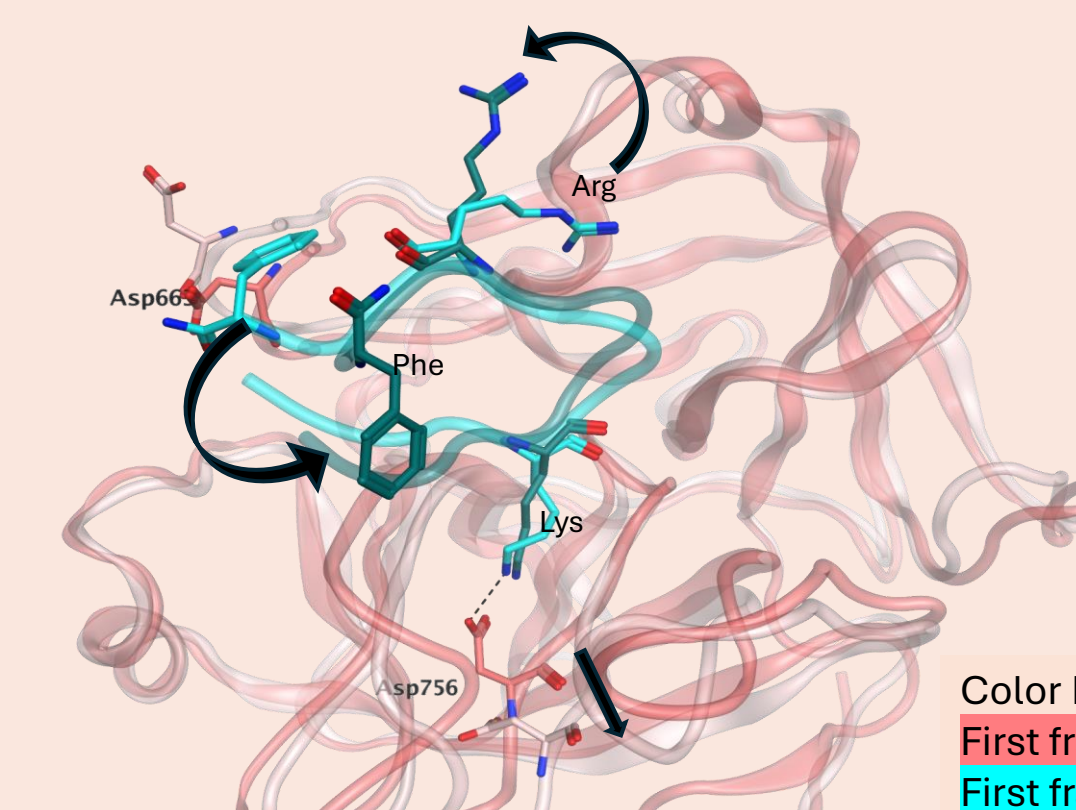
**strong MT1 inhibitor  $K_i = 8.5$  nM**  
**weak MT2 inhibitor  $K_i = 7900$  nM**

Moreover, this inhibitor has presented unprecedented specificity toward MT1 as compared to MT2. The  $K_i$  value was almost **1000-times lower for MT1 than for MT2**. To the best of our knowledge, such significant selectivity, combined with high inhibitory potency, have not been reported so far, for any known MT1 inhibitors.

Molecular dynamic (MD) study was applied to explain significant difference in binding of the inhibitor with MT1 and MT2.



Color key:  
First frame MT1 Last frame MT1  
First frame inhibitor Last frame inhibitor



Color Key:  
First frame MT2 Last frame MT2  
First frame inhibitor Last frame inhibitor

- MT1**
- the P1 inhibitor's Lys<sup>5</sup> forms a stable hydrogen bond with the MT1 Asp799 at the bottom of S1 pocket
  - the inhibitor's Arg<sup>10</sup> forms a hydrogen bond interaction with the MT1 Arg662 (not present in MT2)
  - initially, the inhibitor's C-terminal Phe<sup>13</sup> is in close distance to the MT1 Phe706 in S4 pocket (first frame), however, after reaching a stable conformation, the C-terminal tail bends towards the MT1 active site (last frame)
- MT2**
- the P1 inhibitor's Lys<sup>5</sup> don't form a hydrogen bond with the MT1 Asp756 in S1 pocket
  - Asp756 relocates from its initial position, moving away from the inhibitor's P1 Lys<sup>5</sup>
  - initially, the inhibitor's C-terminal Phe<sup>13</sup> is located in close distance to the MT2 Asp663 in S4 pocket and after reaching a stable conformation, the tail bends towards the MT1 active site

MD study has underscored dynamic behavior of the inhibitor's C-terminal tail. It was shown that the inhibitor's Phe<sup>13</sup> moves from the MT1 hydrophobic region towards the active site. As a result, an expected and potentially favorable interaction between Phe<sup>13</sup> and Phe706 benzene rings has been abolished.

Our goal was to verify experimentally these MD findings. Hence, the Phe<sup>13</sup> was substituted with various proteinogenic and non-proteinogenic amino acids including (Fig.1): (i) amino acids more hydrophobic than Phe which may provide stronger interactions with Phe706; (ii) more hydrophilic such as Lys; (iii) as well as Gly deprived of any side chain (considered as control).

## RESULTS

Table.1 List of synthesized peptides

Name	Inhibitor sequence
H	Gly-Cys(&)-Trp-Thr-Lys-Ser-Ile-Pro-Pro-Arg-Pro-Cys(&)-Phe-NH <sub>2</sub>
H-1	Gly-Cys(&)-Trp-Thr-Lys-Ser-Ile-Pro-Pro-Arg-Pro-Cys(&)-DPhe-NH <sub>2</sub>
H-2	Gly-Cys(&)-Trp-Thr-Lys-Ser-Ile-Pro-Pro-Arg-Pro-Cys(&)-diPhe-NH <sub>2</sub>
H-3	Gly-Cys(&)-Trp-Thr-Lys-Ser-Ile-Pro-Pro-Arg-Pro-Cys(&)-Bpa-NH <sub>2</sub>
H-4	Gly-Cys(&)-Trp-Thr-Lys-Ser-Ile-Pro-Pro-Arg-Pro-Cys(&)-PheTrt-NH <sub>2</sub>
H-5	Gly-Cys(&)-Trp-Thr-Lys-Ser-Ile-Pro-Pro-Arg-Pro-Cys(&)-PheF-NH <sub>2</sub>
H-6	Gly-Cys(&)-Trp-Thr-Lys-Ser-Ile-Pro-Pro-Arg-Pro-Cys(&)-Bip-NH <sub>2</sub>
H-7	Gly-Cys(&)-Trp-Thr-Lys-Ser-Ile-Pro-Pro-Arg-Pro-Cys(&)-NPhe-NH <sub>2</sub>
H-8	Gly-Cys(&)-Trp-Thr-Lys-Ser-Ile-Pro-Pro-Arg-Pro-Cys(&)-PheNO <sub>2</sub> -NH <sub>2</sub>
H-9	Gly-Cys(&)-Trp-Thr-Lys-Ser-Ile-Pro-Pro-Arg-Pro-Cys(&)-Gly-NH <sub>2</sub>
H-10	Gly-Cys(&)-Trp-Thr-Lys-Ser-Ile-Pro-Pro-Arg-Pro-Cys(&)-Trp-NH <sub>2</sub>
H-11	Gly-Cys(&)-Trp-Thr-Lys-Ser-Ile-Pro-Pro-Arg-Pro-Cys(&)-Lys-NH <sub>2</sub>
H-12	Gly-Cys(&)-Trp-Thr-Lys-Ser-Ile-Pro-Pro-Arg-Pro-Cys(&)-NMePhe-NH <sub>2</sub>
H-13	Phe-Cys(&)-Trp-Thr-Lys-Ser-Ile-Pro-Pro-Arg-Pro-Cys(&)-Phe-NH <sub>2</sub>

& - cyclization, disulfide bridge

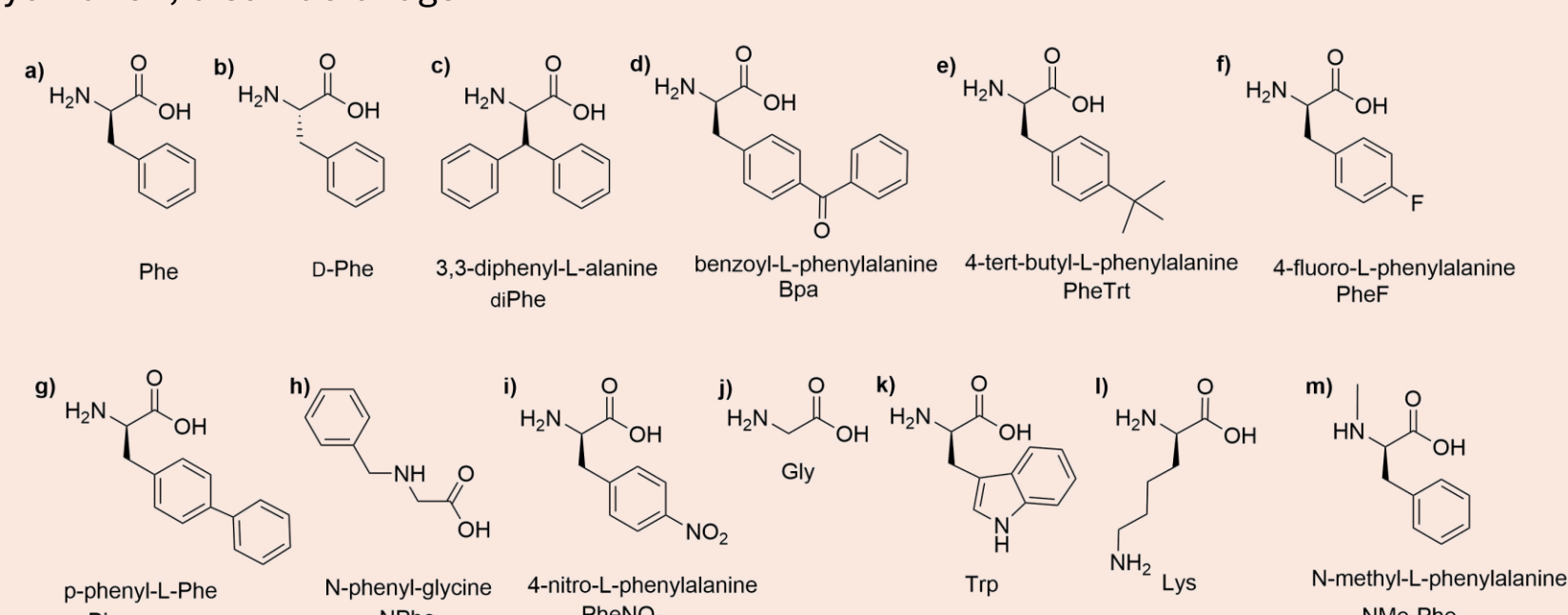


Fig.1 Amino acids introduced instead of Phe<sup>13</sup>

## METHODS

Peptides were synthesized using Fmoc/tBu chemistry on Rink Amide resin. The peptide chain was elongated in the consecutive cycles of deprotection and coupling. Deprotection was performed with 20% piperidine in DMF, and peptide chains elongation was done using 3-fold molar excess of each Fmoc-protected amino acid, TBTU/HOBt/NMM (molar ratio 1:1:1.2). After completing the synthesis, peptides were cleaved from the resin and the protecting groups were removed in a one-step procedure using a mixture of TFA:phenol:triisopropylsilane:H<sub>2</sub>O (88:5:2:5, v/v/v/v). The disulfide bridge was formed using a 0.1 M methanolic iodine solution. Crude compounds were purified by reverse-phase high performance liquid chromatography (RP-HPLC) on PLC 2050 Gilson HPLC with Grace Vydac C18 HPLC column (22 × 250 mm, 10 μm, 300 Å). The solvent system was 0.1% TFA (A) and 80% acetonitrile in A (B). The purity of each peptide was checked by RP-HPLC on a Shimadzu Prominence-1 LC-2050C 3D equipped with a Kinetex XB-C18 column (150 × 4.6 mm, 5 μm) and a UV-Vis detector. A linear gradient 10%-90%B for 20 min, flow rate 1 mL min<sup>-1</sup>, and detection at 214 nm was used. The mass spectrometry analysis was carried out on MALDI MS (Autoflex maX MALDI-TOF spectrometer, Bruker Daltonics).

The activities of the purified, recombinant enzymes were assessed using fluorogenic substrate Boc-QAR-MCA by Fluostar Omega plate reader (BMG Labtech) with an excitation wavelength of 360 nm and emission wavelength 450 nm. The IC<sub>50</sub> values (inhibitor concentrations giving 50% inhibition) were calculated using a four parameter fit model (GraFit Erithacus Software Ltd). The K<sub>i</sub> values were calculated using the Cheng-Prusoff equation, assuming the competitive mode of inhibition, according to the following relationship: IC<sub>50</sub> = K<sub>i</sub>(1+S/K<sub>m</sub>) where K<sub>m</sub> is Michaelis constant (48 μM), S is substrate concentration 10 μM. Enzyme concentration was 0.25 nM.

Molecular dynamic study: MT1 (PDB ID: 3P8F) and MT2 (Homology model). The homology model was constructed starting from the published crystal structure of MT1 [3]. GROMACS: MD simulation; 500 ns. MOE: Analysis and Visualization. The method was validated using SFTI-1 – MT1 complex (PDB:3P8F). "The first frame" and "The second frame" refer to the initial and last molecular dynamics poses of the inhibitors in the active sites of the MT1 and MT2 receptors.

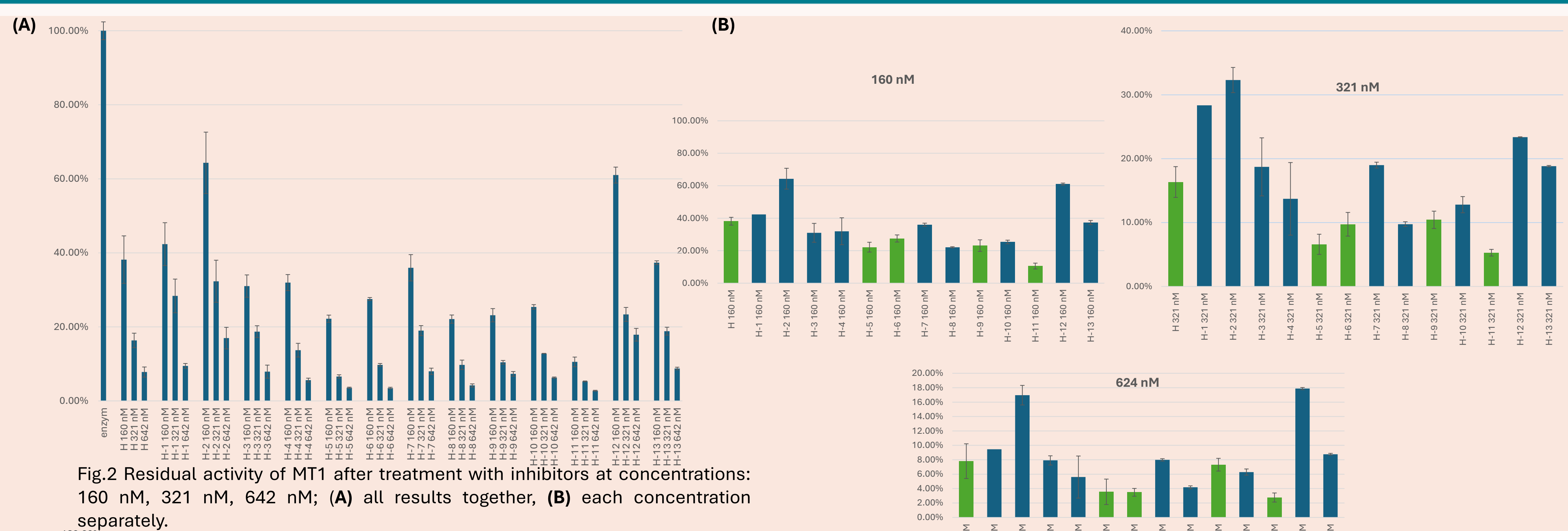


Fig.2 Residual activity of MT1 after treatment with inhibitors at concentrations: 160 nM, 321 nM, 642 nM; (A) all results together, (B) each concentration separately.

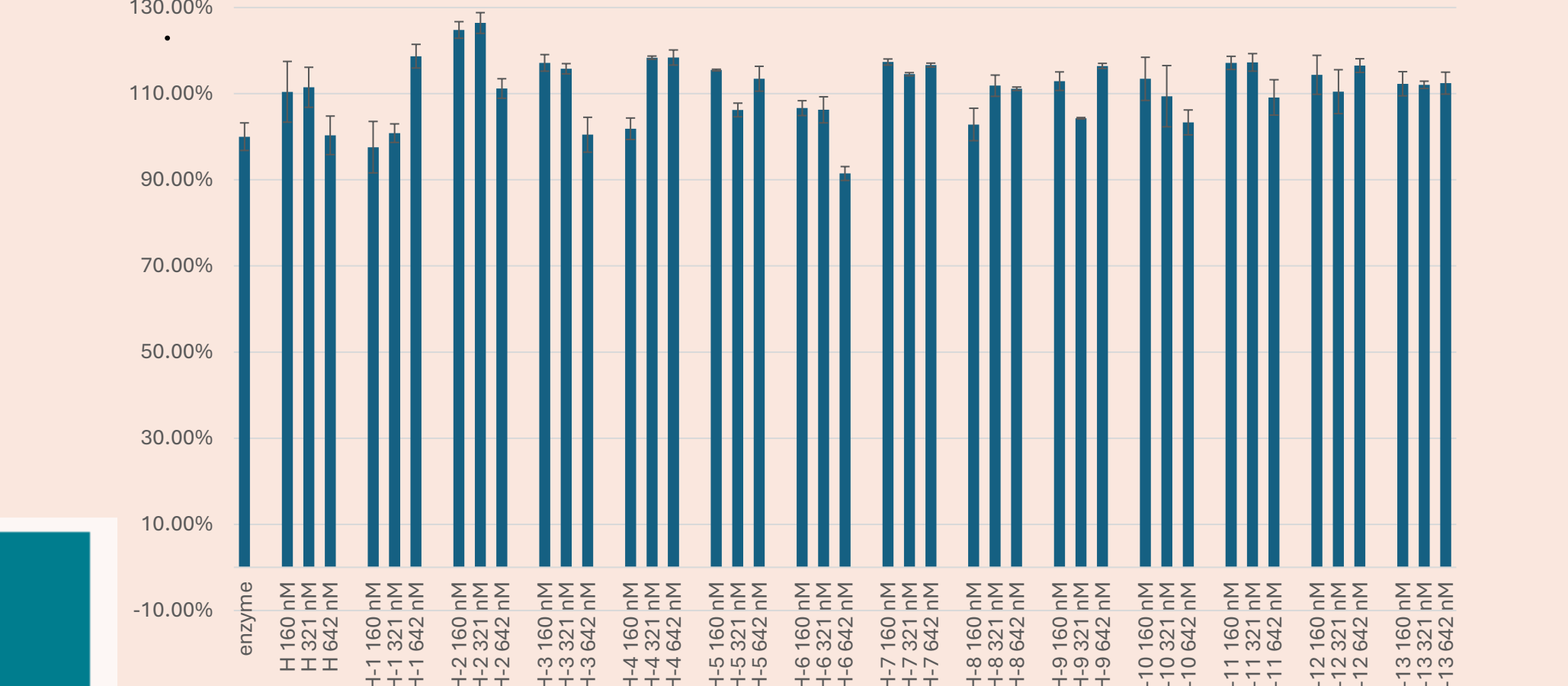


Fig.3 Residual activity of MT2 after treatment with inhibitors at concentrations: 160 nM, 321 nM, 642 nM.

Table 2. IC<sub>50</sub> and K<sub>i</sub> values measured for the selected most active inhibitors.

analog	AA in 13	nM	
		IC <sub>50</sub>	K <sub>i</sub>
H	Phe	31.60±4.6	26.15±3.81
H-5	PheF	16.80±1.20	13.90±0.99
H-6	Bip	17.60±1.30	14.57±1.08
H-9	Gly	33.10±2.70	27.39±2.23
H-11	Lys	19.30±1.10	15.97±0.91

## CONCLUSIONS

- Despite various C-terminal modifications, all inhibitors retained inhibitory activity towards MT1 (Fig.2) and significant specificity – they did not block MT2 (Fig.3)
- Peptides H-5 (PheF<sup>13</sup>), H-6 (Bip<sup>13</sup>) and H-11 (Lys<sup>13</sup>) are stronger inhibitors of MT1 than the parent peptide H; their K<sub>i</sub> values are almost 2 times lower than that of peptide H with Phe<sup>13</sup> (Table 2)
- High, almost the same activity of H-6 with hydrophobic and bulky 4-phenyl-phenylalanine (Bip<sup>13</sup>) and H-11 with hydrophilic Lys<sup>13</sup> may be regarded as an experimental confirmation of MD study that pointed out dynamic behavior of C-terminal tail.
- High activity of H-11 and weak activity of H-2 with hydrophobic, spatial diPhe<sup>13</sup> question the role of interaction between C-terminal inhibitor's tail and hydrophobic Mat1 S4 pocket surrounded by Phe703, Phe706, Phe708, and Trp826. This is consistent with MD study showing that the C-terminal tail appears to distance itself from this region and change its surroundings.
- It may be speculated that surprising difference in inhibitory activity between H-2 (low activity) and H-6 (high activity) is related to different space hindrances caused by diPhe<sup>13</sup> and Bip<sup>13</sup>, rather than to, for example, entropic penalty.
- MD study underscores the importance of intramolecular hydrogen bonding, including interaction between the amide group of C-terminal Phe<sup>12</sup> and carbonyl oxygen of Trp<sup>3</sup>, which stabilize specific inhibitor's conformation more conducive for binding to the enzyme. Low inhibitory activity of peptide H-12 with N-methylated Phe confirms this finding. N-methylated Phe is unable to form such interaction. However, the importance of intramolecular hydrogen bonding is challenged by peptide H-7 having NPhe (due to side chain C→N shift is unable to form hydrogen bond) which presents activity comparable to that of parent peptide H.
- Further MD study are necessary to explain the reported results.

## REFERENCES

1. Murza A., et al (2020) Inhibitors of Type II transmembrane serine proteases in treatment of diseases of the respiratory tract. Expert Opinion on Therapeutic Patents. 30(11): 807-824.
2. Gitlin-Domagalska, A., Dębowski, D., et al. (2020) Truncation of *Huia Versabilis* Bowman-Birk Inhibitor Increases Its Selectivity, Matriptase-1 Inhibitory Activity and Proteolytic Stability. Biochimie, 171-172, 178-186.
3. St-Georges, C. et al. (2017) Modulating the Selectivity of Matriptase-2 Inhibitors with Unnatural Amino Acids. Eur. J. Med. Chem., 129, 110-123.